

Determinations of the Strong Coupling at HERA

T. Schörner-Sadenius
*Deutsches Elektronen-Synchrotron (DESY),
 Notkestr. 85,
 22607 Hamburg,
 Germany*

The status of determinations of the QCD coupling constant, α_s , at HERA is reviewed. Since jet final states provide the most relevant input to the HERA determinations of α_s , the relevant methods used in and results from jet physics are also discussed. Furthermore, HERA and world averages of α_s values are presented. Finally, the HERA-PDF 1.6 proton parton distribution function set which also uses jet final-state data is introduced.

1. INTRODUCTION

The world's only ep collider, HERA at DESY, Hamburg, concluded operations in 2007 after 15 years of data taking. Until then, integrated luminosities of about 0.5 fb^{-1} had been collected by each of the two colliding-beam experiments H1 and ZEUS. An integral part of the HERA physics programme are studies of the hadronic final state, often in the shape of hard hadronic jets, with the aim of testing predictions of (perturbative) QCD (pQCD). Consequently, much effort has gone into extractions of the strong coupling constant, α_s , from jet measurements.

Values of α_s have also been extracted from inclusive measurements which are sensitive to α_s and to the gluon density in the proton, g , only via scaling violations. Furthermore, in these measurements g and α_s are strongly correlated. The corresponding results on α_s are therefore less precise than those from jets. One way out of this problem is to include jet data in fits of the proton *parton distribution functions* (PDFs), thus introducing leading-order sensitivity to g and α_s and adding quark-induced contributions to the cross section which break the strong g - α_s correlation mentioned above. A recent PDF fit result making use of this feature comes from the HERA-PDF working group (HERA-PDF 1.6).

This article reviews measurements of the strong coupling constant at HERA, with an emphasis on the relevant jet measurements, on combinations of α_s values and on combined extractions of the PDFs and α_s .

to 27.5 GeV. The proton beam energy was raised from 820 to 920 GeV towards the end (1998) of the “HERA-I” data-taking phase which lasted until 2000. With these beam energies, HERA achieved a centre-of-mass energy of about 318 GeV. A shutdown in the years 2001–2003 was used to prepare the HERA-II phase which brought an increase in luminosity by a factor 4–5 and the possibility of longitudinal lepton polarisation.

The HERA experiments H1 and ZEUS were typical high-energy physics detectors. The most striking feature of both detectors was their asymmetric structure which reflected the different beam energies of proton and lepton beam and the boosted centre-of-mass system. Both H1 and ZEUS provided tracking with silicon detectors close to the interaction point and large-volume jet drift chambers. Typical p_T resolutions were of the order of $\sigma(p_T)/p_T = 0.006 \cdot p_T [\text{GeV}]$ for both experiments. The tracking devices were surrounded by calorimeters (LAr sampling technology with 45 000 cells and lead / steel absorbers in H1, depleted uranium with scintillator for the compensating ZEUS calorimeter with about 12 000 cells). The energy resolutions for electrons were determined in test beam measurements to be $11(18)\%/\sqrt{E [\text{GeV}]}$ for electrons in the case of H1 (ZEUS). For hadrons, the ZEUS performance was about $35\%/\sqrt{E [\text{GeV}]}$, for H1 $50\%/\sqrt{E [\text{GeV}]}$ were achieved.

2. EXPERIMENTAL ENVIRONMENT

The HERA ep collider¹ was in operation from 1992–2007. The electron beam energy was fixed

¹ HERA could accelerate both electrons and positrons. Since the lepton charge sign is of no importance for the physics discussed here, the term “electron” will be used generically for both electrons and positrons.

In both experiments, superconducting coils provided magnetic fields of 1.16(1.43) T (H1 / ZEUS). The experiments were additionally equipped with small-angle detectors for the measurement of particles close to the beam pipe, and with large-area muon chambers for the rejection of cosmic-ray background and the measurement of muons and hadronic leakage. Luminosity detectors which employed the Bethe-Heitler (or *bremssstrahlung*) process $ep \rightarrow ep \gamma$ complemented the detectors.

3. QCD AND PHYSICS AT HERA

3.1. QCD and the Strong Coupling

The strong coupling constant α_s is the central parameter of QCD. It obeys the *renormalisation group equation* (RGE)

$$Q^2 \frac{\partial \alpha_s(Q^2)}{\partial Q^2} = \beta(\alpha_s(Q^2)) . \quad (1)$$

The β function can be calculated using perturbative methods; so far contributions up to four-loop precision have been derived. The solution for α_s at the two-loop level (which is the relevant one for usage in NLO pQCD calculations of jet cross sections) is given by

$$\alpha_s(Q^2) = \frac{1}{\beta_0 L} - \frac{1}{\beta_0^3 L^2} \beta_1 \ln L , \quad (2)$$

with known coefficients $\beta_{0,1}$ and $L = \ln(Q^2/\Lambda^2)$. Λ defines the energy scale at which the perturbative approach breaks down. Its value has to be determined from data and is of the order of 200 MeV.

The RGE fixes the behaviour of α_s with energy scale but not the absolute normalisation which has to be taken from data. Alternatively, one can fix the coupling value for a given reference energy scale μ and express the value at other scales Q^2 as a function of the reference scale. For the one-loop solution this leads to

$$\alpha_s(Q^2) = \frac{\alpha_s(\mu^2)}{1 + \alpha_s(\mu^2) \beta_0 \ln \frac{Q^2}{\mu^2}} . \quad (3)$$

Typically the reference scale μ is chosen to be the mass of the Z boson, M_Z . Equation 3 can be used to evolve the strong coupling from the scale M_Z — at which it is often measured — to any arbitrary scale that might be needed in a calculation.

3.2. Basics of HERA Physics

Figure 1 (left) shows a Feynman diagram for a lowest-order ep scattering process. The incoming electron with four-momentum k interacts with the proton (momentum P) via the exchange of a boson of four-momentum q , resulting in a final state with a scattered lepton (k') and a hadronic final state X . The kinematics of this process are fully described by the following quantities: The *momentum transfer* $Q^2 = -q^2 = -(k - k')^2$ defines the resolution power of the exchanged boson. The *Bjorken scaling variable* $x = Q^2/(2P \cdot q)$ defines the proton's momentum fraction that participates in the hard interaction. The *inelasticity* $y = (P \cdot q)/(P \cdot k)$ is the fractional energy transferred from the electron to the proton in the latter's rest frame. The quantities Q^2 , x and y are related via the squared centre-of-mass energy, s ,

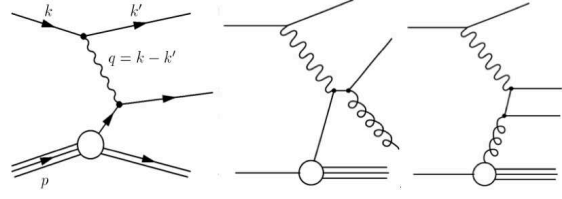


Figure 1: Feynman diagrams of important processes in ep physics.

such that for given beam energies two of the three are sufficient to fully characterise the kinematics of the scattering process: $Q^2 = xys$.

Two further distinctions are made: First, the observable Q^2 is used to define two different kinematic regimes: *photoproduction* (PHP) is defined by the condition $Q^2 \sim 0$; for Q^2 significantly larger than 1 GeV² one speaks of *deep-inelastic scattering*. Second, the type of the exchanged boson is used to distinguish between *neutral-current* (NC, for electron / Z -boson exchange) and *charged-current* (CC, W^\pm -boson exchange) events. In the latter case, the final-state lepton is a neutrino and will escape the experiment undetected, leading to missing transverse energy in the final state. For determinations of the strong coupling constant at HERA, CC jet physics is of negligible importance.

The kinematics of the ep scattering are typically derived from measurements of the scattered electron or, in the case of CC events or of photoproduction events (where the electron escapes the experiment undetected), from the properties of the hadronic final state.

The hadronic final state was originally calculated from the energy depositions in the calorimeters. Later on, *energy-flow algorithms* were developed in both experiments which aim at maximising the resolution by making the best use of both tracking and calorimetric information. Also jets were either reconstructed from calorimeter cells (mostly for ZEUS) or from the energy-flow objects (typically in H1). The hadronic energy scale is known, in both experiments, to about 1%, and this uncertainty is in most cases the dominating experimental one, followed often by the model uncertainty that is evaluated by using different MC models for the correction of the data for detector effects.

The experiments at HERA typically measure the so-called *reduced cross section*, σ_r , that is close related to the double-differential cross section in the kinematic quantities Q^2 and x and that is to a good approximation given by the structure function F_2 :

$$\sigma_r = \frac{1}{Y_\pm} \frac{d^2 \sigma_{NC}^\pm}{dx dQ^2} \frac{x Q^4}{2\pi\alpha^2} = F_2(1 + \Delta) , \quad (4)$$

with $Y_\pm = 1 \pm (1 - y)^2$.

In leading order, F_2 is related to the PDFs — or more precisely the quark densities, $q_i(x, Q^2)$ — via the relation $F_2 = x \sum_i e_i^2 (q_i + \bar{q}_i)$, where the sum runs over all quark flavours and e_i is the charge of the quark i in units of the elementary charge. From a measurement of F_2 , therefore, the PDFs can be extracted using the DGLAP evolution equations.

At HERA, the HERA-PDF working group has since a few years extracted PDF sets from combined H1+ZEUS reduced cross section data. The latest HERA-PDF set based entirely on inclusive (structure-function) data is known as HERA-PDF 1.5 [1].

3.3. Jet Physics at HERA

The inclusive measurements sketched above rely exclusively on the measurement of the scattered electron and the subsequent determination of the kinematics. Neither is the hadronic final state involved, nor does the leading-order contribution (left diagram in figure 1) involve a QCD coupling — the process is of a purely electroweak nature —, nor do the inclusive data provide a direct access to the gluon density in the proton, g (an indirect access that is also strongly correlated with α_s is given via the scaling violations of the DGLAP evolution equations). All these limitations for more extensive studies of QCD can be overcome by studies of jets.

Jets are (collimated) bundles of hadrons which are created by the showering and hadronisation of final-state partons. Since the involved processes do not lead to significant transverse momenta, the resulting hadrons are close in phase space. A jet is formed from these hadrons by applying a specific procedure or *jet algorithm* that defines which particles are combined into a jet and how the resulting jet four-momentum is calculated from the four-vectors of the contributing particles. The limited transverse momenta also ensure that the jet's four-momentum is close to the original parton's so that the jets can be regarded as the “footprints” of the final-state partons and can give direct access to the hard interaction. At HERA, typically the *longitudinally invariant inclusive k_T algorithm* [2] is used. For DIS analyses, the algorithm is typically applied in the *Breit reference frame* in which the transverse momenta of the jets are a measure for the hardness of the underlying QCD process.

The two Feynman diagrams in the centre and on the right side of figure 1 show the dominant contributions to jet production at HERA; they are of order $\mathcal{O}(\alpha_s)$ (centre: *QCD-Compton process* or QCDC; right: *boson-gluon fusion* or BGF). The BGF process introduces a dependence of the jet production cross section on the gluon density, g , already at leading order. The QCDC process, on the other hand, helps to break the aforementioned strong correlation between the gluon density and α_s from which inclusive mea-

surements suffer.

The cross section for jet production can be written as a convolution of the proton PDFs $f_{i/p}$ with a hard scattering matrix element $\hat{\sigma}$, expanded in powers of α_s :

$$\sigma_{\text{jet}} = \sum_n \alpha_s^n (\mu_r^2) \cdot \sum_{i=q,\bar{q},g} \int dx f_{i/p}(x, \mu_f^2) \cdot C_{i,n}(x, \mu_r^2, \mu_f^2). \quad (5)$$

In this equation, the f_i are the parton distribution functions, and the coefficients C_i can be calculated — up to some order — in pQCD. The μ_r and μ_f are the renormalisation and factorisation scales. The terms proportional to α_s^2 or higher correspond to corrections to the leading-order diagram. In pQCD, jet cross sections can be calculated up to next-to-leading order (NLO) for the case of inclusive-jet, dijet and tri-jet production (DIS) or dijet production (PHP). Measurements of jet cross sections have been performed for all of these scenarios in various regions of phase space (different regions of Q^2 , various requirements on transverse energies or pseudorapidities of the jets, etc.). The dominating theoretical uncertainty (and often the largest uncertainty overall) is typically the effect of unknown higher orders (beyond NLO) in the perturbative expansion. This uncertainty is typically estimated by a variation of the renormalisation scale, μ_r , in the calculations.

4. THE STRONG COUPLING AT HERA

4.1. Deriving the Strong Coupling at HERA

Two different methods for deriving the strong coupling from HERA jet data exist. ZEUS [3] typically performs NLO QCD calculations with PDF sets that use different input α_s values, making it possible to parametrise the dependence of the theory cross section in a given analysis bin i of an observable A on α_s by a quadratic function:

$$\left. \frac{d\sigma}{dA} \right|_i = C_1 \cdot \alpha_s(M_Z) + C_2 \cdot \alpha_s^2(M_Z). \quad (6)$$

The cross section measured in bin i is then mapped to the parametrisation and the value of α_s can easily be read off. In this way, the full coupling dependence of the PDFs and the hard scattering matrix element is preserved, and experimental and theoretical uncertainties can easily be derived. The method is applicable to both single data points and to sets of several points.

H1, on the other hand, employs the Hessian method [4] for deriving values of α_s . In this method

a full χ^2 is evaluated for an arbitrary number of data points:

$$\chi^2 = \vec{V}^T \cdot M^{-1} \cdot \vec{V} + \sum_k \epsilon_k^2, \quad (7)$$

where the matrix M comprises the statistical and uncorrelated systematic uncertainties and $V_i = \sigma_i^{exp} - \sigma_i^{theo} (1 - \sum_k \Delta_{ik} \epsilon_k)$. The σ_i are the measured and theoretically predicted cross sections for bin i , Δ_{ik} is the correlated systematic uncertainty of type k for bin i , and ϵ_i is a fit parameter which in equation (7) is used as a penalty term. The experimental uncertainty can be read off at the places where $\chi^2 = \chi_{min}^2 + 1$. The Hessian method is also used in the combined HERA α_s determinations discussed below.

4.2. α_s from PHP Jet Data

ZEUS recently released a preliminary determination of α_s from a PHP measurement of inclusive-jet cross sections in 300 pb $^{-1}$ of HERA-II data [5]. The result of the measurement is shown in figure 2 as a function of the transverse jet energy, E_T . The measurement is experimentally limited by the jet energy scale uncertainty which amounts to 1.8% on the extracted values of $\alpha_s(M_Z)$; the theoretical uncertainties are dominated (as is the case for most HERA jet measurements) by the influence of missing higher orders in the perturbative expansion of the cross section. The effect on α_s is estimated to be of the order of 2.5%. The resulting value for α_s is

$$\alpha_s(M_Z) = 0.1206^{+0.0023}_{-0.0022} (exp)^{+0.0042}_{-0.0033} (theo) .$$

A similar measurement [6] in slightly smaller statistics (189 pb $^{-1}$) has also been carried out using the anti- k_T and SISCONe jet algorithms (instead of only the k_T algorithm) which are by now the default choices at the LHC. Compatible values of the strong coupling have been extracted from all three measurements.

4.3. α_s from DIS Jet Data

In PHP jet measurements, the transverse jet energy, E_T , is used as a hard scale. In DIS, also the photon virtuality Q^2 can be used (or linear combinations of E_T and Q^2). However, at low values of Q^2 , the theoretical uncertainty due to the effect of missing higher orders in the perturbative expansion is typically significant.

H1 measured inclusive-jet, dijet and trijet cross sections at low values of Q^2 between 5 and 100 GeV 2 in HERA-I data [7]. The measurements were performed (multi-)differentially as functions of e.g. Q^2 and jet p_T . As a first step, values of α_s have been extracted from all 61 measured data points individually. The individual values are observed to be well compatible.

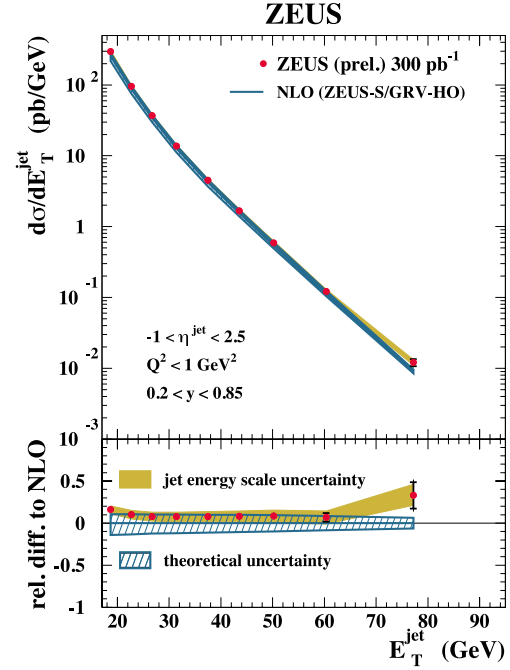


Figure 2: ZEUS inclusive-jet cross section in PHP compared to NLO predictions.

In a next step, combinations of all data points in 4 different Q^2 intervals were fitted. Since the experimental uncertainties of the resulting α_s values are typically much smaller than the theoretical ones, the results demonstrate the limited predictive power of NLO calculations at least at low Q^2 values and thus the necessity of going to higher orders in the perturbative expansion, i.e. of using calculations at next-to-next-to-leading order (NNLO).

Finally, all 61 data points are included in one combined fit, resulting in an α_s value of

$$\alpha_s(M_Z) = 0.1160 \pm 0.0014 (exp)^{+0.0093}_{-0.0077} (theo) \pm 0.0016 (PDF) .$$

The di- and trijet cross sections just discussed were also used by the H1 collaboration for a measurement of the strong coupling from the ratio $R_{3/2}$ of trijet to dijet cross section. A possible benefit of this ratio is a (partial) cancellation of some systematic uncertainties between numerator and denominator (luminosity, scales, PDFs ...). However, the result alone is not competitive with the best determinations from e.g. inclusive-jet cross sections at high Q^2 (see later). A similar analysis has also been performed by ZEUS [8].

4.4. α_s at the Highest Q^2 Values

In a 2009 publication, H1 continued the low- Q^2 measurement of inclusive-, di- and trijets described above in the high- Q^2 regime (above 150 GeV 2) [9]. Figure 3 shows the main result, namely the running

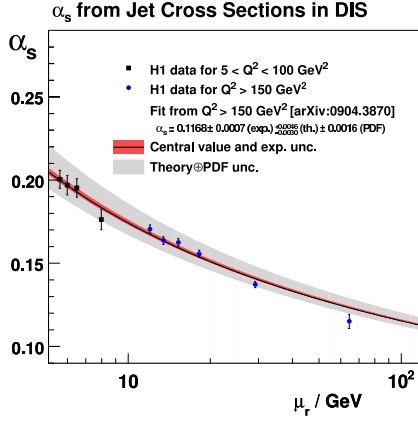


Figure 3: H1 α_s values from combinations of 1/2/3-jet cross sections in high- and low- Q^2 measurements.

of the coupling as derived from a combined fit to all high- Q^2 data points (solid line with error band), together with individual α_s values (evolved to their respective scale) at high Q^2 (small circles). In the figure, the high- Q^2 α_s determination is extrapolated down to the low- Q^2 regime of the measurement described above. The good agreement of the extrapolation with the four low- Q^2 measurements (small squares) is as striking as is the strong reduction of the theoretical uncertainties with respect to the low- Q^2 α_s result.

It is due to this smaller sensitivity to theoretical uncertainties that most α_s measurements at HERA have been performed in the region of high Q^2 values. The most recent published ZEUS and H1 results comprise a measurement of inclusive-jet cross sections at $Q^2 > 125 \text{ GeV}^2$ with the k_T , anti- k_T and SISONE jet algorithms in 82 pb^{-1} of HERA-I ZEUS data, and a multi-differential measurement measurement of inclusive/di/tri-jet cross sections in 351 pb^{-1} at $Q^2 > 150 \text{ GeV}^2$ from H1.

The ZEUS measurement [10] used the $d\sigma/dQ^2$ distributions at Q^2 values above 500 GeV^2 for the extraction of the strong coupling, since this region proved to have the smallest theoretical uncertainties. The agreement observed between data and NLO QCD is excellent, and up to Q^2 values of about 1000 GeV^2 the theory uncertainty is found to dominate the measurement. ZEUS extracted a value of the strong coupling for each of the three jet algorithms; the three values are very well compatible, and the k_T result is given as

$$\alpha_s(M_Z) = 0.1207 \pm 0.0014 (\text{stat}) \\ +0.0035 \text{ } ^{+0.0022}_{-0.0033} (\text{exp}) \text{ } ^{+0.0022}_{-0.0023} (\text{theo}) .$$

The analysis has also been repeated in about 300 pb^{-1} of HERA-II data [11], and the two results agree very well.

The latest H1 high- Q^2 measurement [12] was the first H1 jet measurement to profit from a strongly improved calibration of the hadronic final state and jet

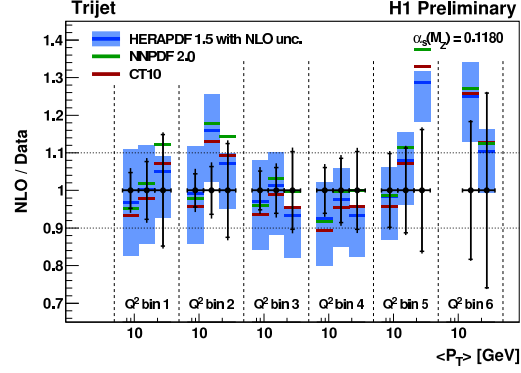


Figure 4: H1 ratio of trijet cross sections to NLO predictions in different regions of Q^2 as functions of the average jet p_T .

energy scale. In addition, the statistics of 351 pb^{-1} were large enough to allow the first double-differential measurement of trijet cross sections to be performed. As in the low- Q^2 case, H1 extracted α_s values from each measured data point of the (average) p_T distributions for inclusive jets, dijets and trijets in different regions of Q^2 . The individual measurements agree very nicely as can be seen in figure 4 which shows the resulting α_s values for the trijet cross sections for different average jet p_T values and Q^2 regions. Typically, the scale uncertainties are larger than the experimental uncertainties by a factor of about 2.

In a next step, again, α_s values are extracted from a combined fit to all data points within a certain Q^2 region, and from all combined inclusive-/di/tri-jet data points. As it turns out, the value extracted from the trijet data points offers the smallest experimental uncertainty. This is due to the fact that the trijet cross section already at leading order is proportional to α_s^2 . The resulting value is

$$\alpha_s(M_Z) = 0.1196 \pm 0.0016 (\text{exp}) \\ \pm 0.0010 (\text{PDF}) \text{ } ^{+0.0055}_{-0.0039} (\text{theo}) ;$$

the inclusive-jet and dijet results are compatible.

4.5. Alternatives: α_s from Jet Shapes

Jet final states offer still more accesses to the strong coupling value than only via the cross-section measurements discussed above. One example is a ZEUS extraction of α_s from the averaged integrated jet shape, $\langle\psi(r)\rangle$, in DIS [13]. The quantity $\langle\psi(r)\rangle$ is defined as $\langle\psi(r)\rangle = \frac{1}{N_{jets}} \sum_{jets} \frac{E_T(r)}{E_T^{jet}}$, where N_{jets} is the number of jets studied, $E_T(r)$ is the transverse energy contained in a cone of radius r ($0 < r < R$, with the jet radius R) around the jet axis, and E_T^{jet} is the total jet transverse energy. $\langle\psi(r)\rangle$ is thus a measure for the distribution of transverse energy inside a

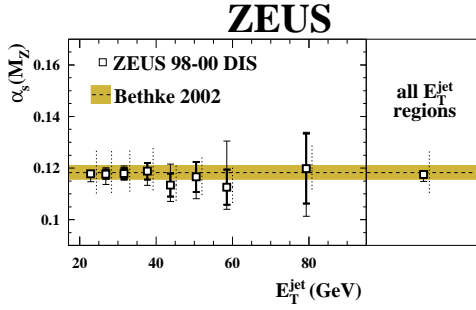


Figure 5: ZEUS α_s values extracted from integrated jet shapes at radius 0.5 as a function of E_T^{jet} .

jet, and an understanding of this quantity gives interesting insights into the fragmentation process and allows, among other things, gluon and quark jets to be discriminated against each other on a statistical basis.

For the extraction of α_s , ZEUS parametrised the cross section for $\langle\psi(r)\rangle$ at a radius $r = 0.5$ in different bins of E_T^{jet} as $\langle\psi(r)\rangle = C_1 + C_2 \cdot \alpha_s(M_Z)$. The constants C_i were taken from a fit to the theoretically predicted cross section at different values of $\alpha_s(M_Z)$. Since the predictions include only terms of order $\mathcal{O}(\alpha_s)$, a reduced sensitivity to α_s is obtained:

$$\alpha_s(M_Z) = 0.1176 \pm 0.0009 (\text{stat}) \\ +0.0009 (\text{exp})^{+0.0091}_{-0.0026} \text{ (theo)} .$$

Figure 5 shows the α_s values extracted for the individual E_T^{jet} bins and for the combined extraction.

5. THE HERA α_s COMBINATIONS

Since 2004, the HERA collaborations have started to combine their α_s measurements [14]. Since 2007, combined fits to H1 and ZEUS data sets have been performed using the Hessian method. The 2007 HERA average, which was based on an inclusive-jet $d\sigma/dQ^2$ measurement from ZEUS and the double-differential inclusive-jet $d^2\sigma/dE_T dQ^2$ from H1, resulted in [15]

$$\alpha_s(M_Z) = 0.1198 \pm 0.0019 (\text{exp}) \pm 0.0026 (\text{theo}) .$$

Again, the result is dominated by the theory uncertainties, underlining the necessity of higher orders in the jet cross-section calculations.

Figure 6 [14] shows a compilation of α_s measurements from H1 and ZEUS at their respective energy scales. The data points demonstrate the excellent agreement between results obtained from various jet final states, from different kinematic regimes (DIS and PHP), and with different methods (H1 and ZEUS). Furthermore, the running character of the coupling can be demonstrated with data from one experimental

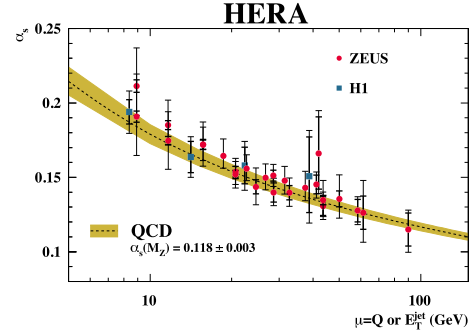


Figure 6: Demonstration of running of α_s from HERA jet measurements.

environment alone — and it is in excellent agreement with the running as predicted by QCD based on the world average of α_s (solid line, see also later).

6. COMBINED FITS OF PDFS AND α_s

As indicated above, fits to the inclusive structure-function measurements alone provide good insight into the proton structure, but only poorly constrain α_s . In addition, there are regions in phase space which are not sufficiently covered by structure-function data to meaningfully constrain the PDFs. One example is the gluon density at large values of x . Here, the use of jet data might help: First, the jet data provide sensitivity to g already at leading order, and specifically at large x , and second, the QCD contributions to the jet cross sections break the strong correlation between gluon density and α_s , allowing a meaningful determination of both parameters to be done simultaneously.

This insight had early impacts e.g. in a 2005 ZEUS publication [16] in which both structure-function data and DIS and PHP jet cross sections were used in PDF fits, leading to the ZEUS-JETS PDF set. The result was a competitive determination of α_s and a reduction of the uncertainty on the gluon density at medium and large values of x of up to 35%.

This idea was recently taken up by the HERA-PDF working group who also included jet data from H1 and ZEUS into their PDF fits, leading to the HERA-PDF 1.6 set [17]. Detailed studies with fixed α_s as in HERA-PDF 1.5 showed that the inclusion of the jet data does not change the resulting PDF fit very much, the most remarkable difference being the behaviour of the gluon density at high x which becomes slightly softer. Freeing α_s in the fit, however, for the case of HERA-PDF 1.5 suffers from the already mentioned gluon- α_s correlation which increases the error on the gluon density. Here HERA-PDF 1.6 (with jets) is clearly superior, with much smaller uncertainties on the gluon density as can be seen from figure 7 which shows, at the top, HERA-PDF 1.5 as a function of x

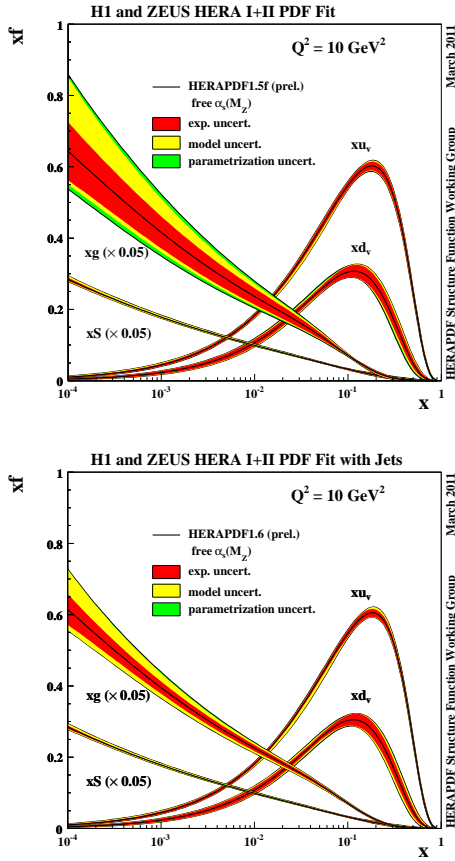


Figure 7: Comparison of HERA-PDF 1.5 (top) and 1.6 (bottom).

and at the bottom HERA-PDF 1.6 for $Q^2 = 10 \text{ GeV}^2$.

The HERA-PDF 1.6 value for α_s of

$$\alpha_s(M_Z) = 0.1202 \pm 0.0013 (\text{exp}) \pm 0.0007 (\text{model}) \pm 0.0012 (\text{hadronisation})^{+0.0045}_{-0.0036} (\text{scale})$$

is comparable to the HERA 2007 average discussed above.

7. HERA AND α_s WORLD DATA

Figure 8 shows a comparison of the α_s value obtained from HERA-PDF 1.6, from the included individual jet measurements from H1 and ZEUS, and the world average [18]. There is excellent agreement, although of course the world average has significantly smaller uncertainties.

In fact, the precision in the world average value (of order 1%) comes mostly from the very precise derivations of α_s from lattice calculations [19] and from the analysis of τ decays. Among the high-energy collider α_s values contributing to the world average, the determinations from HERA are very competitive.

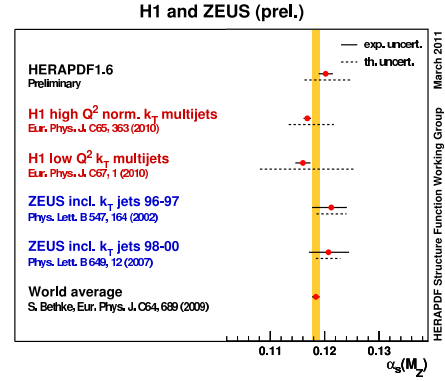


Figure 8: Comparison of different α_s values, including the one from HERA-PDF 1.6.

8. CONCLUSIONS

HERA has contributed massively to our current understanding of QCD, and in particular to the world knowledge of the proton structure and the central parameter of QCD, α_s . Values for α_s have been derived both in analyses of structure functions and from jet measurements in DIS and PHP. Lately, the H1 and ZEUS collaborations have also begun to derive combined values of α_s from their data sets and to derive values for α_s in PDF fits which take both inclusive structure-function and jet data into account. The HERA α_s values are an important input to the α_s world average.

References

- [1] R. Placakyte, these proceedings.
- [2] S.D. Ellis *et al.*, Phys. Rev. D **48** 1993 3160.
- [3] E.g. ZEUS Collab., Phys. Lett. B **547** (2002) 164.
- [4] M. Botje, Eur. Phys. J. C **14** (2000) 285.
- [5] ZEUS Collab., ZEUS-prel-11-005.
- [6] ZEUS Collab., ZEUS-prel-10-015.
- [7] H1 Collab., Eur. Phys. J. C **67** (2010) 1.
- [8] ZEUS Collab., Eur. Phys. J. C **44** (2005) 183.
- [9] H1 Collab., Eur. Phys. J. C **65** (2010) 363.
- [10] ZEUS Collab., Phys. Lett. B **691** (2010) 127.
- [11] ZEUS Collab., ZEUS-prel-10-002.
- [12] H1 Collab., H1prelim-11-032.
- [13] ZEUS Collab., Nucl. Phys. B **700** (2004) 3.
- [14] C. Glasman, he-ex/0506035.
- [15] H1 and ZEUS Collab., H1prelim-07132 and ZEUS-prel-07-025.
- [16] ZEUS Collab., Eur. Phys. J. C **42** (2005) 1.
- [17] H1 and ZEUS Collab., H1prelim-11-034 and ZEUS-prel-11-001.
- [18] S. Bethke, Eur. Phys. J. C **64** (2009) 689.
- [19] C. Davies, these proceedings.